Am J Cancer Res 2025;15(6):2890-2904
www.ajcr.us /ISSN:2156-6976/ajcr0164281

Original Article

Enhanced inhibitory effects of mianserin in combination with sorafenib on liver cancer growth through targeting the CCR9-AKT pathway

Ya-Hui Huang[1,2*], Chia-Jung Liao[3*], Meng-Han Wu[3], Ming-Wei Lai[1,4], Yung-Hsin Yeh[5,6], Chau-Ting Yeh[1,2], Yang-Hsiang Lin[1], Kwang-Huei Lin[1,3,7]

[1]Liver Research Center, Chang Gung Memorial Hospital, Linkou Main Branch, Taoyuan, Taiwan; [2]Molecular Medicine Research Center, Chang-Gung University, Taoyuan, Taiwan; [3]Graduate Institute of Biomedical Sciences, College of Medicine, Chang-Gung University, Taoyuan, Taiwan; [4]Division of Pediatric Gastroenterology, Department of Pediatrics, Chang Gung Memorial Hospital Linkou Main Branch, Taoyuan, Taiwan; [5]Department of Cardiovascular, Chang-Gung Memorial Hospital, Tao-Yuan, Taiwan; [6]Department of Medicine, College of Medicine, Chang Gung University Tao-Yuan, Tao-Yuan, Taiwan; [7]Center for Drug Research and Development, College of Human Ecology, Chang-Gung University of Science and Technology, Taoyuan, Taiwan. [*]Equal contributors.

Received March 2, 2025; Accepted April 21, 2025; Epub June 25, 2025; Published June 30, 2025

Abstract: Previously, our group showed that mianserin, an atypical antidepressant, exerts stronger cytotoxicity against liver cancer cells than normal hepatocytes, supporting its potential application as a therapeutic agent for liver cancer. However, the anti-tumor effects of mianserin *in vivo* and its mechanisms are yet to be established. In this study, we explored the inhibitory effects and mechanisms of mianserin and evaluated its efficacy in combination with sorafenib against liver cancer cells. Effects on cell viability were assessed via MTT and flow cytometry assays and antitumor activity evaluated using a xenograft model. Changes in the expression and distribution of specific proteins within cells were examined via immunoblot assay. Our results indicate that mianserin exerts cytotoxic effects by inhibiting cell viability through suppression of proliferation and induction of apoptosis. Therapeutic effects of mianserin were validated via intratumoral injection in the xenograft model. Mechanistically, our data indicate that mianserin-induced cytosolic HSP60 translocates to cell surface and participates in the downregulation of CCR9, leading to inactivation of the AKT-(β-catenin/NFκB) signaling pathway. Combination treatment with mianserin and sorafenib induced significant synergistic effects on cell viability, apoptosis, and *in vivo* tumor growth in both parental and sorafenib-resistant liver cancer cells. This study is the first to demonstrated that mianserin effectively limits the growth of liver cancer by downregulating CCR9, in turn, inactivating the AKT-(β-catenin/NFκB) pathway. Both *in vitro* and *in vivo* experiments highlight mianserin's potential as an adjuvant therapy to sorafenib, offering a promising strategy to overcome current challenges in liver cancer treatment.

Keywords: Liver cancer, mianserin, sorafenib, HSP60, CCR9, AKT

Introduction

Hepatocellular carcinoma (HCC) is the fifth most common cancer type in men and seventh in women worldwide [1]. Despite several available treatment options [2], the disease remains the fourth leading cause of cancer-related mortality due to phenotypic diversity and high recurrence rates, highlighting the urgent ongoing need to develop novel and innovative therapeutic strategies and drugs in this context.

Antidepressants are primarily used for the treatment of mental disorders. With the exception of some atypical antidepressants, these compounds are generally classified as selective serotonin reuptake inhibitors (SSRI), serotonin and norepinephrine reuptake inhibitors (SNRI), tricyclic antidepressants (TCA), and monoamine oxidase inhibitors (MAOI), based on the mechanism of action. Accumulating studies have demonstrated that specific antidepressants can exert anti-tumor effects against different types of cancers including HCC. For

https://doi.org/10.62347/CYDE4091

example, desipramine (TCA) and fluoxetine (SSRI) exert anti-proliferative effects by inducing apoptosis in Hep3B cells [3, 4], while amitriptyline (TCA) induces mitochondrial dysfunction in HepG2 cells [5]. In keeping with the results obtained from cell studies, an Asian population-based study in 2017 revealed that TCAs and SSRIs are associated with lower risk of HCC [6]. In 2018, another population-based case-control study similarly reported association of SSRIs (including fluoxetine, sertraline, paroxetine, citalopram, escitalopram and fluvoxamine) with lower HCC risk [7].

In addition to TCA- and SSRI-mediated inhibition of liver cancer cell proliferation, we previously observed that mianserin, an atypical antidepressant, exerts more pronounced cytotoxic effects on liver cancer cells than normal human hepatocytes, indicating a novel capacity to inhibit growth of liver cancer [8]. However, the inhibitory effects of mianserin *in vivo* and its underlying mechanisms of action are yet to be fully elucidated. The main objective of the present study was to establish the inhibitory impact of mianserin on liver cancer cell viability and associated mechanisms, both *in vitro* and *in vivo*. In addition, the effects of combined treatment with mianserin and sorafenib on the viability of parental and sorafenib-resistant liver cancer cells were assessed.

Materials and methods

Cell culture, antibodies, and reagents

HepG2 and J7 cells were obtained from The Bioresource Collection and Research Center (BCRC) of the Food Industry Research and Development Institute, Hsinchu, Taiwan, and Dr. C. S Yang, National Taiwan University, Taiwan, respectively [9]. The authenticity of the cell line was confirmed through a short tandem repeat-based assay utilizing the Promega StemElite ID System. HepG2 and J7 cells were cultured in Dulbecco's modified Eagle's medium (DMEM) supplemented with 10% fetal bovine serum (FBS) within a humidified incubator maintained at 37°C and 5% CO_2. Antibodies against cyclin D1, AKT, and p-AKT (Ser473) were obtained from Cell Signaling (Danvers, MA, US), CDK4 and β-catenin were sourced from Abcam (Cambridge, UK), HSP60 from Proteintech Group (Taipei, Taiwan), and NFκB from Millipore Corp (Burlington, MA, US). Mianserin and sorafenib were procured from MedChemExpress (Monmouth Junction, NJ, US) and CCL25 from PeroTech™ (Waltham, MA, US). For *in vitro* experiments, mianserin (20 mg/mL) and sorafenib (10 mM) were dissolved in dimethyl sulfoxide (DMSO) to prepare stock solutions. Concentrations approximating the IC50 values of mianserin [8] and sorafenib (Figure S1) were used in the subsequent cell model experiments. A solution of mianserin dissolved in PBS at a concentration of 0.05 mg/mL was utilized for animal experiments.

MTT assay

Cells were plated in 48-well culture plates and incubated overnight. At specific time-points following treatment with mianserin (10 μg/ml) and/or sorafenib (5 μM for HepG2 cells and 6 μM for J7 cells), thiazolyl blue tetrazolium bromide (MTT; Sigma-Aldrich, St. Louis, MO, US) was added to the culture plates. After 4 h, solubilization solution (10% SDS in 0.01 M HCl) was introduced for cell lysis, and the reaction allowed to proceed overnight. The cell proliferation index was determined by quantifying the optical density at 570 nm against a reference wavelength of 650 nm using a microplate reader.

Immunoblot assay

Cells were plated and incubated overnight. At specific time points following treatment with mianserin (10-40 μg/ml for 24-72 h) and/or sorafenib (5 μM for 24-48 h), cells were subjected to protein extraction. Concentrations of protein extracts were quantified by using the Bradford assay. Based on the abundance of each target, adequate amount of proteins were separated on a 10% SDS-polyacrylamide gel and subsequently transferred to PVDF membranes, followed by incubation with primary antibodies for 1 h. After removal of the primary antibodies, membranes were incubated with horseradish peroxidase-conjugated secondary antibodies for subsequent ECL signal detection (Immobilon Western Chemiluminescent HRP Substrate, Millipore). Protein signals were detected using X-ray film and quantified with Image Gauge 3.46 software (FUJIFILM, Tokyo, Japan). The quantification results were supplemented in Table S1.

Apoptosis assay

HepG2 and J7 cells were cultured in the absence or presence of mianserin (20 μg/mL) and/or sorafenib (8 μM) for 48 h. Cells were stained with fluorescein isothiocyanate (FITC)-conjugated annexin V and PI for 30 min at room temperature using an Annexin V:FITC Apoptosis Detection Kit (BD Pharmingen, San Diego, CA, US) prior to flow cytometry analysis. Signals were detected using a FACSCalibur flow cytometer (Becton Dickinson, Franklin Lakes, NJ, US) and data analysis conducted using the Modfit LT program (Verity Software House, Brunswick, ME, US).

Subcutaneous xenograft animal model

Five-week-old male nude mice (BALB/c) were inoculated with parental (J7) or sorafenib-resistance (J7-SR) cells (1×10^6/100 μL PBS) via subcutaneous injection on the flank. Once tumors reached a size of 250 mm^3, mice were randomly assigned to control or treatment groups. The mouse model used a range of 1-60 mg/kg of mianserin for intraperitoneal injection [10, 11]. Considering the regional effect and low systemic effects of intratumoral administration, we started mianserin treatment at 2-3 mg/60 μl/mouse (approximately 100-150 mg/kg) in the animal model. Mice in the mianserin treatment group received intratumoral injections of mianserin five days a week. The experiment was concluded on day 7 or 14, and the animals were terminated by CO_2 asphyxiation according to the guideline published by American Veterinary Medical Association. Mice in the sorafenib treatment group received sorafenib orally three times a week (30 mg/kg body weight). The experiment was concluded on day 7. Tumor volume (mm^3) was calculated using the formula: W × L × T (W, smallest diameter; L, longest diameter; T, thickness). All animal experiments were conducted in accordance with the standards approved by the Institutional Animal Care and Use Committee of Chang Gung University (CGU110-096, CGU111-153). This institution holds a valid AAALAC accreditation.

Subcellular fractionation and immunoprecipitation assay

Cells were plated and incubated overnight. At specific time points following treatment with mianserin (10-20 μg/ml for 16-72 h), cells were subjected to subcellular fractionation and/or immunoprecipitation assay. The Mitochondria Isolation Kit (Thermo Scientific, Waltham, MA, US) was used for isolation of cytosol and mitochondria and the Mem-PER Plus Membrane Protein Extraction Kit (Thermo Scientific) for the extraction of plasma membrane proteins. All extraction procedures were performed in keeping with the manufacturers' instructions. Isolated plasma membrane proteins obtained were incubated overnight at 4°C with the anti-HSP60 antibody. Pre-reacted Protein A/G-agarose beads (Santa Cruz Biotechnology, Dallas, TX, US) with anti-mouse IgG antibodies were added for 30 min at 4°C before introducing the immune complex. Immunocomplexes were incubated with Protein A/G-agarose beads for 1 h at 4°C and proteins ultimately eluted from the beads using 2× SDS sample buffer for immunoblot analysis.

Establishment of sorafenib-resistant cells

The half-maximal inhibitory concentration (IC50) of sorafenib for liver cancer cells was 6 μM [12]. The initial concentration of sorafenib used for treatment of HepG2 and J7 cells was 5 μM, which was gradually increased by 0.25 μM per week up to a dose of 6 μM (over a period of 5 weeks). The sorafenib-resistant cell lines generated, designated HepG2-SR and J7-SR, were maintained in DMEM containing 10% FBS and 6 μM sorafenib.

Statistical analysis

Data are expressed as mean ± standard deviation (SD) of a minimum of three independent experiments. Statistical analysis was conducted using Student's t-test or one-way ANOVA, with p-value < 0.05 considered statistically significant.

Results

Mianserin inhibits proliferation and induces apoptosis of liver cancer cells

To confirm the anti-growth effects of mianserin, we assessed the proliferation properties of HepG2 and J7 cells treated with 10 μg/mL mianserin for 1, 2, 3, and 4 days using the MTT assay. As depicted in **Figure 1A**, mianserin inhibited cell proliferation in a time-dependent manner. Additionally, expression of the cell cycle regulators, cyclin D1 and CDK4, was

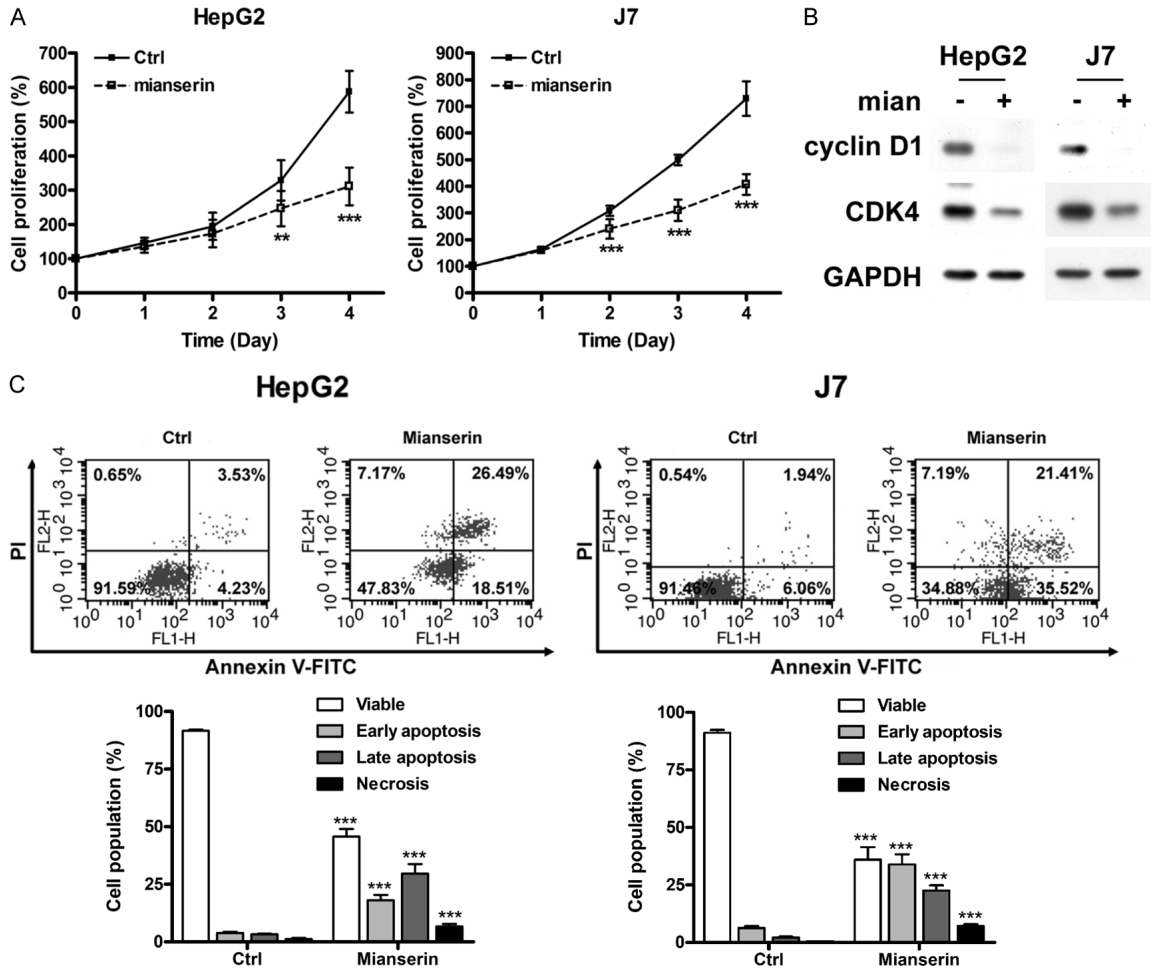

Figure 1. Mianserin inhibits cell growth and induces apoptosis in liver cancer cells. A. Assessment of cell proliferation using the MTT assay. HepG2 and J7 cells were treated with mianserin (10 μg/mL) for 1, 2, 3, and 4 days. B. Immunoblot assay of expression of cyclin D1 and CDK4 in HepG2 and J7 cells following mianserin (mian) treatment. Quantifications of the bands from the representative images are shown. C. Flow cytometry analysis of cell apoptosis. HepG2 and J7 cells were treated with mianserin (20 μg/mL) for 48 h. Representative scatter plots displaying PI (Y-axis) vs. Annexin V (X-axis) are shown. The histogram below the scatter plot illustrates the percentages of viable, early apoptotic, late apoptotic, and necrotic cells. Data are presented as mean ± SD from three independent experiments. ***$P < 0.001$ represents statistical significance compared to the control (Ctrl).

decreased in the two liver cancer cell lines following mianserin treatment (**Figure 1B**). To determine whether mianserin specifically exerts effects on apoptosis in liver cancer cells, flow cytometry-based detection with annexin V-FITC/PI staining was conducted. As shown in **Figure 1C**, treatment with 20 μg/mL mianserin for 48 h induced both early and late apoptosis in HepG2 and J7 cells. The percentage of apoptotic cells (early- and late-stage) increased from 7.13 ± 0.45% to 47.60 ± 2.87% in HepG2 cells and 8.37 ± 1.3% to 56.50 ± 6.12% in J7 cells following exposure to mianserin (**Figure 1C**, lower panel).

Mianserin inhibits tumor growth in the J7 subcutaneous xenograft animal model

Subsequently, the growth inhibitory effects of mianserin on liver cancer *in vivo* were investigated. Based on our previous experience, J7 cells demonstrated superior tumor growth efficiency in xenograft models compared to HepG2 cells. For this reason, J7 cells were chosen for the subcutaneous xenograft experiments. The protocol for the animal experiment is outlined in **Figure 2A**. When J7 xenograft tumors reached a size of 250 mm^3, mianserin was administered via intratumoral injection five

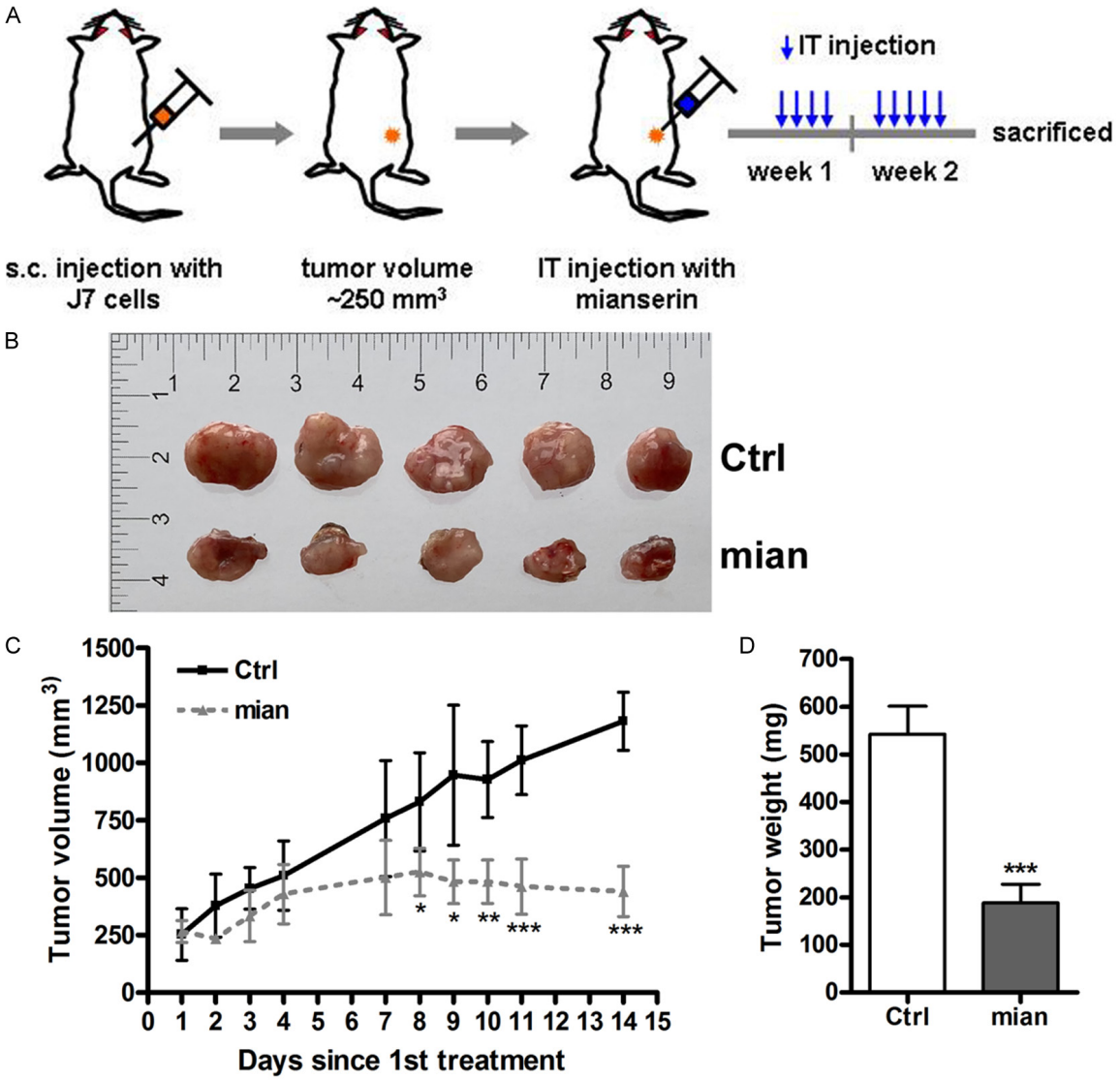

Figure 2. Intratumoral injection of mianserin suppresses tumor growth in the J7 xenograft model. (A) Mianserin treatment via intratumoral injection (IT) in a J7 xenograft mouse model. (B) Final xenograft tumors of control (Ctrl) and mianserin treatment (mian) groups. (C, D) Comparison of tumor growth rates (C) and tumor weights (D) between control and mianserin groups. *$P < 0.05$; **$P < 0.01$; ***$P < 0.001$.

days a week for a total period of 14 days. Notably, mice receiving mianserin treatment exhibited smaller tumor sizes and slower tumor growth curves compared to the control group (**Figure 2B**, **2C**). Furthermore, tumor weights in the mianserin group were significantly lower than those in the control group (**Figure 2D**).

Mianserin induced the translocation of HSP60 to cell surface and downregulated the expression of CCR9

As depicted in **Figure 1**, mianserin inhibits growth of liver cancer cells by suppressing cell proliferation and inducing apoptosis. In view of the finding that heat shock protein 60 (HSP60) plays a pro-apoptotic role following release from mitochondria into the cytosol [13, 14], we further examined expression of HSP60 in both mitochondria and cytosol of liver cancer cells subjected to mianserin treatment. Unexpectedly, a slight increase in mitochondrial HSP60 (mHSP60) expression was observed concomitant with decreased expression of cytosolic HSP60 (cHSP60) in mianserin-treated HepG2 and J7 cells (**Figure 3A**). Based on the previous finding that HSP60 translocates to the cell surface during apoptosis [15], we hypothesized that decreased

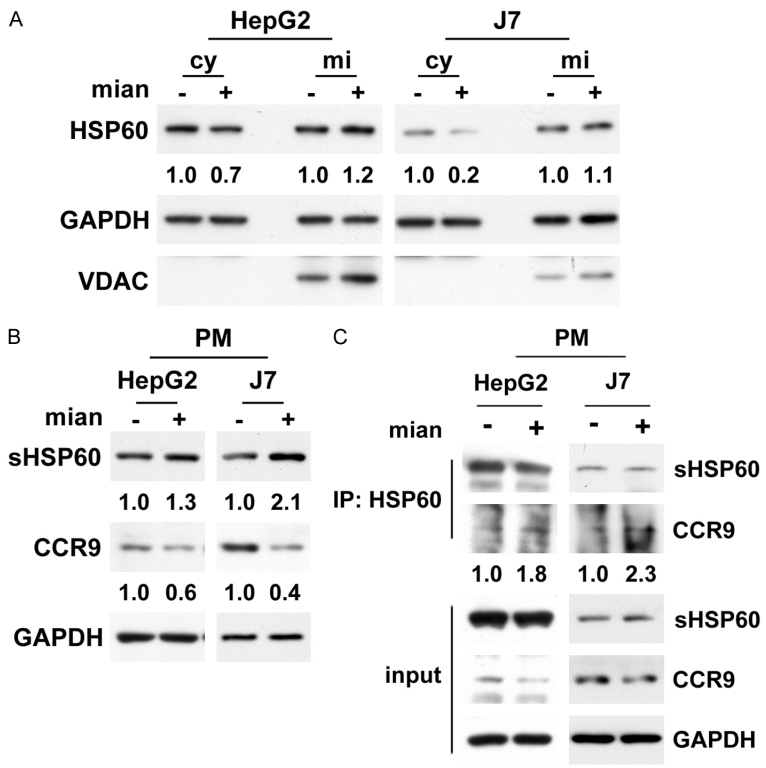

Figure 3. Effects of mianserin on distribution of HSP60 in liver cancer cells. (A, B) Immunoblot assay of HSP60 expression in cytosolic (cy) and mitochondrial (mi) fractions of HepG2 and J7 cells with (+) or without (-) mianserin (10 μg/mL) treatment for 72 h (A). Plasma membrane proteins (PM) were extracted from HepG2 and J7 cells with or without mianserin (20 μg/mL) treatment for 16 h for analysis of sHSP60 and CCR9 expression (B). GAPDH served as the loading control and VDAC as a mitochondrial marker. Quantifications of the bands from the representative images are shown. (C) Plasma membrane proteins (PM) were extracted from HepG2 and J7 cells with or without mianserin (10 μg/mL) treatment for 16 h. PMs were subjected to immunoprecipitation using an anti-HSP60 antibody, followed by immunoblot with anti-HSP60 and anti-CCR9 antibodies (upper panel). The corresponding input control is shown in the lower panel.

expression of cHSP60 is potentially attributed to its migration to the cell surface. To validate this theory, plasma membrane proteins were isolated from liver cancer cells treated with mianserin for immunoblot analysis. As shown in **Figure 3B**, HSP60 was upregulated in the plasma membrane of mianserin-treated cells. Given that mianserin inhibits cell growth, induces apoptosis, and upregulates cell surface HSP60 (sHSP60) in liver cancer cells, we further postulated that sHSP60 may be associated with cell surface receptors involved in the regulation of proliferation or apoptosis. G protein-coupled receptors (GPCR), constituting the largest superfamily of cell surface receptors, have been identified as potential therapeutic targets for HCC [16]. Here, we focused on C-C chemokine receptor type 9 (CCR9) for further analysis, based on its overexpression in HCC tissues, negative correlation with overall survival, and documented role in promoting cell proliferation as well as tumorigenicity [17]. Notably, expression of CCR9 was decreased in liver cancer cells treated with mianserin (**Figure 3B**). To investigate the potential interactions between sHSP60 and CCR9, we conducted an immunoprecipitation (IP) assay using plasma membrane proteins isolated from liver cancer cells with or without mianserin (10 μg/mL) treatment. Following IP with an anti-HSP60 antibody, we observed an increase in the CCR9 signal in both HepG2 and J7 cells treated with mianserin, as confirmed with immunoblot analysis (**Figure 3C**). Our findings suggest that mianserin promotes interactions between sHSP60 and CCR9.

sHSP60 participates in mianserin-induced downregulation of CCR9

To determine whether sHSP60 contributes to the mianserin-induced reduction of CCR9, HepG2 and J7 cells with stable HSP60 knockdown were generated (**Figure 4A**) and treated with mianserin before plasma membrane extraction. As shown in **Figure 4B**, mianserin treatment induced sHSP60 levels and decreased CCR9 expression (lanes 1 and 2). However, the mianserin-induced reduction of CCR9 was partially reversed upon HSP60 knockdown (lane 4 compared to lane 3). The collective findings support a role of sHSP60 in mianserin-induced downregulation of CCR9 in liver cancer cells.

Mianserin inhibits CCR9-mediated activation of AKT, β-catenin, and NFκB in liver cancer cells

Chemokine ligand 25 (CCL25) serves as a ligand for CCR9. Interactions between these

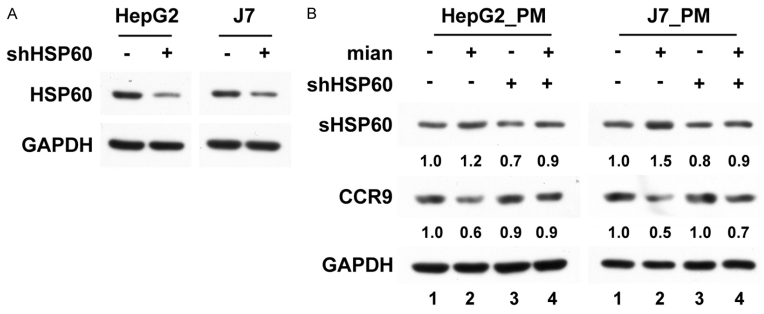

Figure 4. sHSP60 is involved in mianserin-induced downregulation of CCR9 in liver cancer cells. A. Expression of HSP60 in HepG2 and J7 cells with or without HSP60 knockdown. B. PMs were extracted from HCC (HepG2 and J7) cells with or without HSP60 knockdown after treatment with or without mianserin for 16 h. Expression patterns of HSP60 (sHSP60) and CCR9 were examined via immunoblot analysis. Quantifications of the bands from the representative images are shown.

proteins may play a role in cancer progression through activation of various signaling pathways [18]. For example, CCL25/CCR9 interactions are reported to induce chemoresistance through the PI3K-AKT-(β-catenin/NFκB) pathway [18] and trigger anti-apoptotic mechanisms through activation of the PI3K-AKT pathway in tumor cells [18, 19, 20]. Accordingly, we focused on the effects of mianserin on the AKT pathway in liver cancer cells. Exposure of tumor cells to 40 μg/mL mianserin for 24 h led to a decrease in levels of AKT, phospho-AKT (p-AKT), β-catenin, and NFκB (p65) compared to the untreated control group (**Figure 5A**). To further establish the relevance of these changes in molecular expression in relation to CCR9, liver cancer cells with or without CCL25 were treated with mianserin or left untreated. As shown in **Figure 5B**, diminished expression of p-AKT, β-catenin, and NFκB induced by mianserin was partially rescued in cells treated with CCL25 (lane 3 vs. lane 4). Based on these results, we propose that mianserin inactivates p-AKT, β-catenin, and NFκB, potentially through inhibition of CCR9 expression.

Synergistic effects of mianserin and sorafenib on viability and apoptosis of liver cancer cells

Sorafenib, a multi-kinase inhibitor, serves as a frontline treatment for advanced HCC. Previous research has demonstrated that sorafenib promotes activation of the AKT pathway in both parental and sorafenib-resistant (SR) liver cancer cells [21, 22]. Given that mianserin inactivates the AKT pathway, we investigated the effects of combining mianserin with sorafenib on the viability of parental and SR (HepG2-SR and J7-SR) liver cancer cells with the aid of the MTT assay. Doses approximating the IC50 values of mianserin [8] and sorafenib (Figure S1) were applied in the experiments. As shown in **Figure 6A**, treatment of HepG2 cells with 10 μg/mL mianserin or 5 μM sorafenib alone for 3 days resulted in a decrease in cell viability to 62.0% (**Figure 6A**, left panel, slash bars) and 49.8% (**Figure 6A**, left panel, gray bars), respectively, compared to untreated (Ctrl) cells. Notably, combined treatment with mianserin and sorafenib (mian + sora) led to a further reduction in cell viability to 35.5% (**Figure 6A**, left panel, black bars). As expected, HepG2-SR cells displayed a limited response to sorafenib in terms of inhibition of viability relative to HepG2 cells (49.8% forHepG2 vs. 93.5% for HepG2-SR; **Figure 6A**, left panel, gray bars). Mianserin exerted a greater inhibitory effect on the viability of HepG2-SR cells than sorafenib (62.5% (mianserin) vs. 93.5% (sorafenib); **Figure 6A**, left panel, slash bar vs. gray bar), but a comparable inhibitory effect on HepG2 cells (62.0% (HepG2) vs. 62.5% (HepG2-SR); **Figure 6A**, left panel, slash bars). Combined treatment with mianserin and sorafenib still exerted a synergistic inhibitory effect on viability of HepG2-SR cells (50.1%; **Figure 6A**, left panel, black bar). Similarly, the viability of J7 cells co-treated with mianserin (10 μg/mL) and sorafenib (6 μM) was reduced to a more significant extent (to 16.3%) compared to that of counterpart cells treated with mianserin (34.6%) or sorafenib (57.3%) alone (**Figure 6A**, right panel). As expected, sorafenib exerted limited effect on J7-SR cells in terms of inhibition of viability (72.3%) relative to J7 cells (57.3%; **Figure 6A**, right panel, gray bars). Notably, mianserin (34.6% and 50.3%) exerted a greater inhibitory effect on viability of J7 and J7-SR cells than sorafenib (57.3% and 72.3%; **Figure 6A**, right panel). A synergistic inhibitory effect of mianserin and sorafenib on viability (18.2%) was consistently observed in J7-SR cells (**Figure 6A**, right panel, black bar

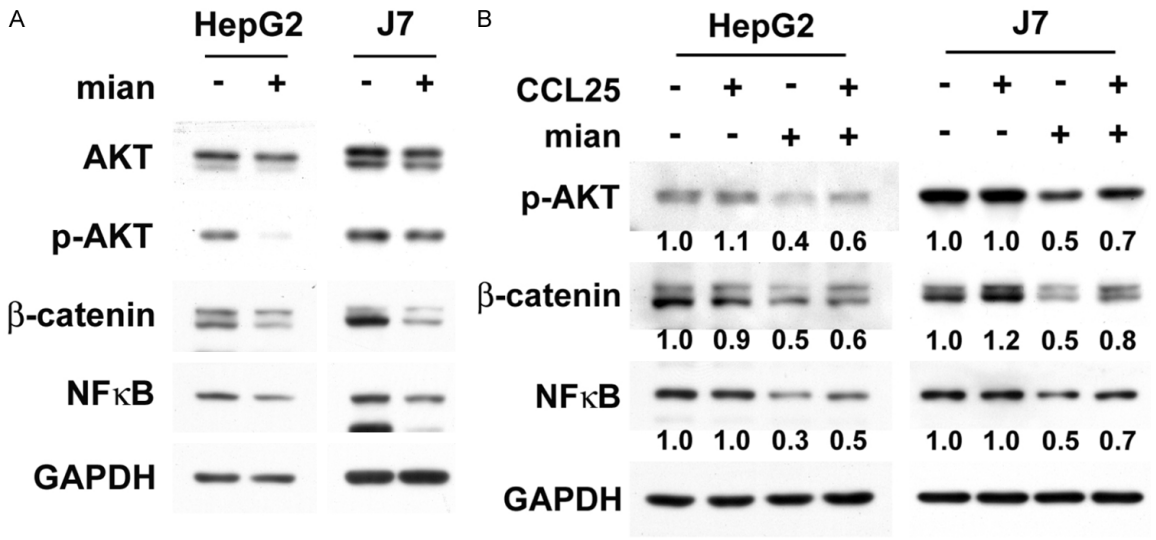

Figure 5. Mianserin inactivates the AKT pathway in liver cancer cells. A. Total proteins were extracted from HepG2 and J7 cells after treatment with mianserin (40 μg /mL) for 24 h and expression of AKT, p-AKT, β-catenin, and NFκB assessed via immunoblot assay. B. Flowing treatment of HepG2 and J7 cells with CCL25 (150 ng/mL for HepG2, 100 ng/mL for J7) or mianserin (15 μg/mL), either alone or in combination, total proteins were extracted for immunoblot evaluation of p-AKT, β-catenin, and NFκB expression. Quantifications of the bands from the representative images are shown.

vs. slash bar and gray bar). Subsequently, apoptosis in J7 and J7-SR cells treated with mianserin (20 μg/mL) or sorafenib (8 μM), either alone or in combination, for 48 h was analyzed via flow cytometry. Both sorafenib (81.46% (J7) and 37.13 (J7SR)) and mianserin (35.48% (J7) and 18.40% (J7-SR)) induced apoptosis in comparison to the corresponding untreated cell groups (8.48% (J7) and 8.12% (J7-SR); **Figure 6B**). Due to the acquisition of resistance by J7-SR cells, the proportion of sorafenib-induced apoptosis was significantly lower compared to J7 cells (37.13% (J7-SR) vs. 81.46% (J7); **Figure 6B**). Interestingly, even with compromised efficacy of sorafenib, a significant synergistic effect was observed upon combination with mianserin in J7-SR cells (93.19% (S + M) vs. 37.13% (S) or 18.4% (M); **Figure 6B**).

Effects of mianserin and sorafenib, alone or in combination, on tumor growth in J7-SR subcutaneous xenograft animal model

According to the results obtained with the cell line model system (**Figure 6A** and **6B**), mianserin induced apoptosis, compromising the viability of J7 and J7-SR cells. Furthermore, mianserin and sorafenib exerted synergistic effects on cell viability and apoptosis, even in J7-SR cells. A J7-SR subcutaneous xenograft model was subsequently employed to determine the efficacy of sorafenib and mianserin, both alone and in combination (**Figure 6C** and **6D**). Tumor growth rates, expressed as percentage tumor volume in relation to the day of treatment initiation (D0), tumor volume (D7) and images of tumors excised from the flank of the mice on the day of sacrifice (D7) are shown. Sorafenib and mianserin, both alone and in combination, induced significant inhibition of tumor growth (**Figure 6C** and **6D**) comparing to untreated group. Mianserin exerted greater tumor inhibitory effects than sorafenib (**Figure 6C** and **6D**). However, only slightly synergistic effects of mianserin in combination with sorafenib were observed in this treatment course.

Discussion

While certain antidepressants, such as fluoxetine and citalopram, have been shown to exert anti-liver cancer effects through different pathways [23], the concept of mianserin as an anti-liver cancer agent had never been proposed until our recent publication in 2023 [8]. In the current study, we conducted additional experiments to validate this theory and to clarify the underlying mechanisms. Our results

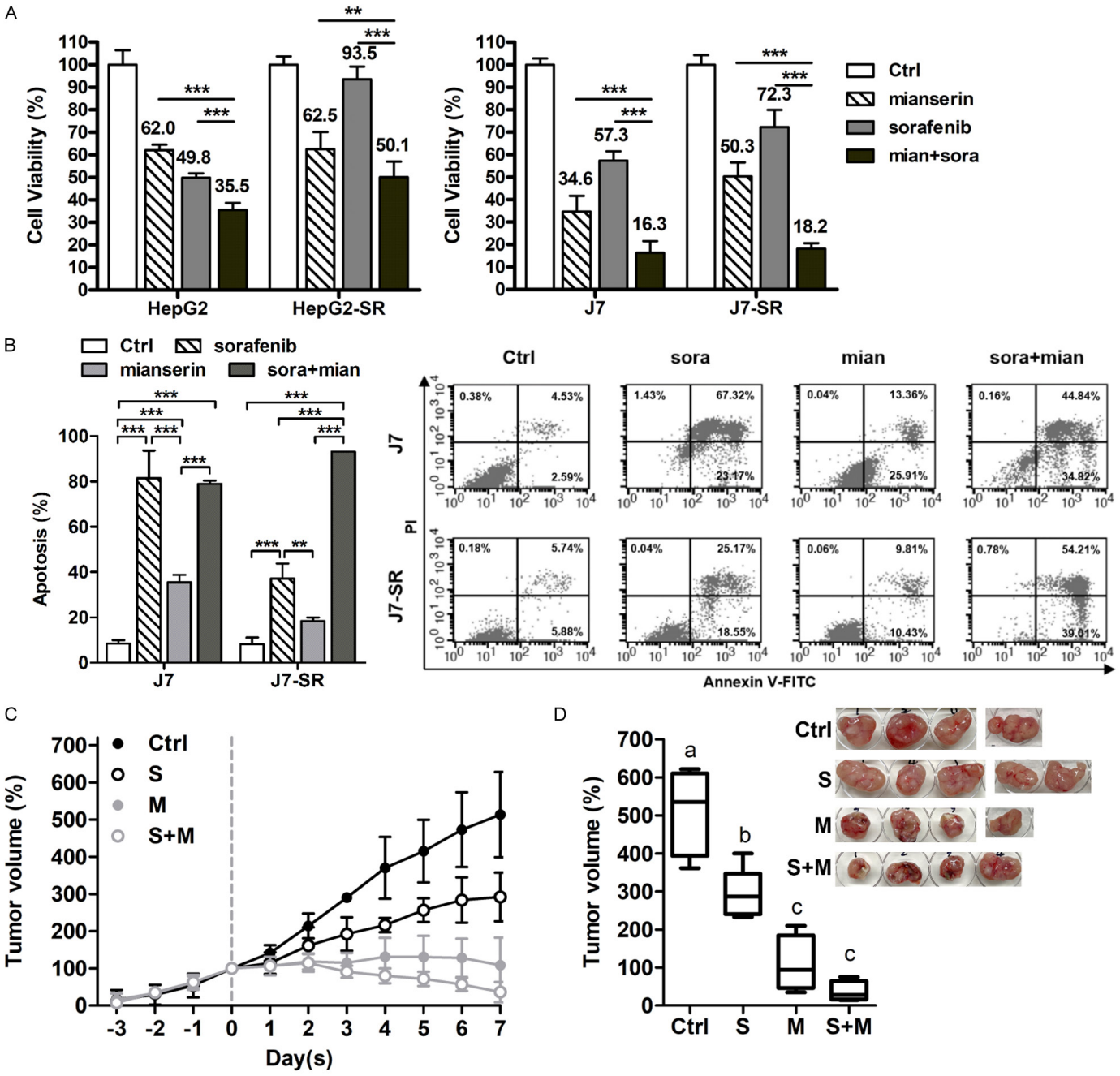
A
Cell Viability (%)
62.0
49.8
35.5
62.5
93.5
50.1
HepG2
HepG2-SR
34.6
57.3
16.3
50.3
72.3
18.2
J7
J7-SR
Ctrl
mianserin
sorafenib
mian+sora
B
Ctrl
sorafenib
mianserin
sora+mian
Apotosis (%)
J7
J7-SR
sora
mian
sora+mian
PI
Annexin V-FITC
0.38%
4.53%
2.59%
1.43%
67.32%
23.17%
0.04%
13.36%
25.91%
0.16%
44.84%
34.82%
0.18%
5.74%
5.88%
0.04%
25.17%
18.55%
0.06%
9.81%
10.43%
0.78%
54.21%
39.01%
C
Tumor volume (%)
Ctrl
S
M
S+M
Day(s)
D
Tumor volume (%)
a
b
c
c
Ctrl
S
M
S+M

Figure 6. Effects of mianserin combined with sorafenib in parental and sorafenib-resistant liver cancer cells. (A) Synergistic effect of mianserin and sorafenib on viability of parental (HepG2 and J7) and sorafenib-resistant (HepG2-SR and J7-SR) liver cancer cells determined using the MTT assay. Data are represented as mean ± SD from three independent experiments and evaluated using one-way ANOVA with Dunnett's T3 (post hoc) analysis. $^{**}P < 0.01$; $^{***}P < 0.001$. (B) J7 and J7-SR cells were treated with sorafenib (8 μM) and mianserin (20 μg/mL), alone or in combination, for 48 h and apoptosis was analyzed using flow cytometry. Quantification results are shown in the left panel, and representative dot plots are shown in the right panel. (C, D) The effects of sorafenib and mianserin on tumor growth were evaluated in a xenograft mouse model. Tumor growth rates are presented as percentage of tumor volume in relation to the treatment -initiation day (D0; C). Tumor volume and images on D7 are shown (D). Bars labeled with different letters (a, b, and c) denote statistical significance (One-way ANOVA with Dunnett's T3 post hoc analysis). Ctrl, vehicle control; S, sorafenib; M, mianserin; S + M, combination treatment with sorafenib and mianserin.

showed that mianserin inhibits the viability of liver cancer cells by suppressing cell proliferation and promoting apoptosis. Additionally, this drug alters the distribution of HSP60, leading to its migration from the cytoplasm to the cell surface and consequent suppression of CCR9 expression in liver cancer cells. Immunoprecipitation experiments further confirmed enhanced interactions between sHSP60 and CCR9 induced by mianserin, and HSP60 silencing experiments provided evidence of the involvement of HSP60 in the decreased expression of CCR9. In view of a previous report that silencing of CCR9 can suppress liver cancer cell growth and tumorigenicity [17], we suggest that mianserin potentially inhibits the viability of tumor cells, by downregulating CCR9.

The mechanisms by which sHSP60-CCR9 interactions induce downregulation of CCR9 remain to be established. Essentially, protein turnover in cells is regulated by the ubiquitin-proteasome system, which involves a multistep process of ubiquitin attachment to the targeted protein for degradation [24]. Accordingly, we speculated that sHSP60-CCR9 interactions activate this system, resulting in the ubiquitination and subsequent degradation of CCR9, which requires further investigation.

Cell cycle dysregulation is a fundamental hallmark of liver cancer development. Cyclin D1 [25] and CDK4 [26], key regulators of the G1/S-phase transition, have been shown to significantly contribute to liver cancer progression. In addition to their role in cell cycle control, modulation of Cyclin D1 and CDK4 expression has been associated with apoptotic regulation [27]. Several anticancer agents, including sorafenib [28], have been demonstrated to induce G1/S-phase arrest and promote apoptosis, underscoring the therapeutic relevance of targeting this checkpoint. Accordingly, we selected Cyclin D1 and CDK4 as representative molecules to evaluate the antiproliferative effects of mianserin. Our study further demonstrated that the PI3K-AKT-(β-catenin/NFκB) signaling axis is a major downstream pathway modulated by CCR9 inhibition following mianserin treatment. Given that AKT signaling regulates Cyclin D1 and CDK4 via transcriptional activation, translational control, and/or protein stability [29, 30], our findings suggest that mianserin may exert its anti-liver cancer effects through modulation of these pathways. Additionally, due to the central role of AKT in cell cycle regulation [30], we acknowledge that other cell cycle regulators may also contribute to the observed anti-proliferative effects of mianserin.

Other than a recent study published in 2022, which reported that mianserin inhibits tumor growth of SW480, a colon adenocarcinoma cell line, by reducing glutamine concentrations [31], no anticancer effects of this compound have been documented. In this study, we confirmed the anti-liver cancer effects of mianserin administered via intratumoral injection into subcutaneous xenograft tumors. Although mianserin has been linked to hepatic injury, liver function returned to normal after the dose was reduced or discontinued [32]. It is important to note that the risk of liver injury from mianserin may be associated with its oral administration route. Interestingly, we tested the cytotoxic effects of low (20 μg/mL, dosage close to IC50) and high (80 μg/mL) doses of mianserin on cancer cells and human hepatocytes in our previous publication [8]. The results revealed that a high dose of mianserin produced significant cytotoxic effect on both cancer cells and human hepatocytes. However, a low dose of mianserin inhibited cancer cell viability (76-90%) more significantly than it

affected human hepatocytes (27.1%). A number of preclinical studies have demonstrated lower systemic toxicity and improved treatment outcomes using the intratumoral administration route [33, 34]. Currently, several clinical trials are underway to investigate the safety and efficacy of intratumoral injection in cancer patients [8]. We consistently observed fewer drug-related side-effects, such as drowsiness, tremors, and weakness, in response to intratumoral injections. Our preclinical findings provide a valuable reference for future clinical research.

While sorafenib has been shown to extend the lives of patients with HCC, the efficacy of the drug is limited by numerous severe side-effects. Additionally, patients commonly develop drug resistance within six months [22]. Therefore, cancer patients would benefit greatly from therapeutic drugs that, when combined with sorafenib, do not cause serious adverse reactions and even allow reduction of the required dose of sorafenib while achieving the same or better therapeutic effects. Previous studies have demonstrated that sorafenib activates the AKT pathway in both parental and SR HCC cells [21, 22, 35, 36]. This phenomenon was also evident in our studies, based on the increased expression of p-AKT in HepG2, HepG2-SR, and J7-SR cells in the presence of sorafenib (Figure S2). Numerous compounds targeting the AKT pathway have been developed and validated as potential cancer therapies in *in vitro* and *in vivo*. For example, the allosteric AKT inhibitor MK-2206 was used to treat sorafenib-resistant liver cancer cells (HepG2-SR and Huh7-SR), which acquire activation of AKT and exhibit epithelial-mesenchymal transition (EMT) [21]. Additionally, the potential of Ipatasertib (GDC0068, an ATP-competitive AKT inhibitor) to reverse sorafenib resistance was studied in liver cancer cells [37]. Ipatasertib synergized with sorafenib in inhibiting tumor growth in the Huh7-SR-injected subcutaneous mouse model. In the current study, similar *in vitro* and *in vivo* results were observed when HepG2-SR and J7-SR cells were treated with sorafenib or mianserin alone or in combination (**Figure 6**). Although several AKT inhibitors have successfully entered clinical evaluation, trials for various cancer types have shown that many AKT inhibitors have limited efficacy as monotherapy [38, 39]. Therefore, exploring the potential of other drugs in combination treatments presents a feasible therapeutic option [40]. Several compounds targeting the AKT pathway have been explored for the management of liver cancer [41]. Among these, MK2206 entered a phase II clinical trial for advanced liver cancer cases that had not responded to prior therapy (NCT01239355). Unfortunately, the study was terminated early due to discouraging results, highlighting the urgent need for innovative therapies targeting the AKT pathway. This study demonstrates that mianserin exhibits liver cancer inhibitory effects in both *in vitro* and *in vivo* experiments and has a synergistic effect with sorafenib, similar to MK-2206 and Ipatasertib. Clinical trials of AKT inhibitors often show limited efficacy and notable side effects [40]. In contrast, mianserin is frequently prescribed to treat depression in cancer patients [42], indicating a favorable safety profile for potential use in clinical trials. However, while mianserin is traditionally administered orally, this study utilized intratumoral injection. Therefore, future research must evaluate the appropriate dosage and administration route to ensure safe and effective cancer treatment. Moreover, this study primarily focuses on the CCR9-AKT pathway. Nevertheless, prior investigations have revealed mianserin's impact on additional signaling pathways, including the G protein coupled receptors pathway [43] and the Wnt pathway [44], which are pivotal in tumor biology. Thus, unlike AKT-specific inhibitors, mianserin might exert tumor control via its multifaceted effects on various pathways, presenting a distinct advantage. Another innovative aspect of this study lies in the drug repurposing strategy involving mianserin, an existing antidepressant with a well-established safety profile. Repurposing offers distinct advantages in terms of time and cost efficiency compared to de novo drug development. Given its clinical history, mianserin-if administered in its conventional oral form-could more readily progress to clinical trials, bypassing many of the safety hurdles typically encountered in early-phase drug development. Furthermore, formulation modifications may be pursued to optimize its pharmacokinetic and pharmacodynamic properties for oncologic applications, potentially accelerating its clinical translation. Our findings provide novel insights into the anticancer potential of mianserin, particularly

in liver cancer, and underscore the importance of further mechanistic studies to delineate its full therapeutic scope. Exploring mianserin's anticancer mechanisms remains a critical avenue for future investigation.

While intratumoral drug administration is a promising strategy for enhancing local efficacy and minimizing systemic toxicity, our study highlights the practical benefits of oral mianserin administration, which has already undergone extensive clinical evaluation for psychiatric use. This route may represent the most feasible approach for rapid clinical implementation. However, this study's lack of direct assessment of oral mianserin constitutes a notable limitation. Despite this, our data strongly support the feasibility of clinical trials investigating oral mianserin as an adjuvant therapy to sorafenib, particularly for preventing or overcoming sorafenib resistance in liver cancer patients. Future directions should include (1) Evaluating the efficacy of oral mianserin in preclinical models of liver cancer; (2) Investigating liver-specific targeting strategies or alternative delivery routes such as intratumoral injection; (3) Conducting mechanistic studies further to elucidate mianserin's molecular targets and signaling pathways; (4) Initiating clinical trials to assess mianserin's therapeutic potential in combination with existing liver cancer therapies. These efforts will be essential for validating mianserin as a viable and innovative therapeutic strategy in liver cancer treatment.

Mianserin inhibits the viability of liver cancer cells, which may be attributed to downregulation of CCR9, leading to inactivation of the AKT-(β-catenin/NFκB) pathway. Our results suggest that the regulation mechanism of mianserin still functions on most AKT-related molecules and CCR9 in SR liver cancer cells compared to their untreated counterparts (Figure S2). Notably, co-treatment of both parental and SR liver cancer cells with mianserin and sorafenib induced greater inhibition of CCR9 and most AKT-related molecules relative to sorafenib treatment alone (Figure S2). Consistently, data from the MTT assay showed that combination treatment with mianserin and sorafenib exerted more pronounced inhibitory effect on the viability of parental and SR liver cancer cells than the individual drug. This synergistic effect on cell apoptosis was additionally observed in J7-SR (**Figure 6B**) but not J7 cells, which could be attributed to the superior effect of sorafenib in J7 cells, thus lessening the difference between treatments. The effects of mianserin and sorafenib on tumor growth were further evaluated in a xenograft animal model. Mianserin displayed significant efficacy, even in sorafenib-resistant J7-SR bearing mice. Combination treatment with mianserin and sorafenib induced a trend of slight increase in inhibition of tumor growth. A well-designed animal study may be important to further to determine the method, dosage, and course of treatment with mianserin as an adjuvant for sorafenib. Overall, evidence of the synergistic inhibitory effects of mianserin and sorafenib obtained from our preliminary *in vitro* and *in vivo* studies provide valuable insights for future clinical applications.

In conclusion, this study validates mianserin's anti-liver cancer potential, demonstrating its ability to inhibit liver cancer cell viability in both *in vitro* and *in vivo* models. Mechanistically, we identified a novel pathway whereby mianserin promotes the translocation of HSP60 from the cytosol to the cell surface, thereby increasing sHSP60 expression and enhancing its interaction with CCR9. This interaction results in the downregulation of CCR9 and subsequent suppression of key downstream signaling effectors, including AKT, phosphorylated AKT (p-AKT), β-catenin, and NFκB. Importantly, our study is the first to demonstrate that mianserin synergistically enhances the anti-tumor efficacy of sorafenib in both parental and sorafenib-resistant liver cancer cells, highlighting its potential as an adjuvant therapy. Key breakthroughs of this study include: (1) The first demonstration of mianserin's anti-liver cancer activity in cell culture and xenograft models. (2) Novel evidence supporting the combination of mianserin and sorafenib as a strategy to inhibit liver cancer progression and potentially overcome sorafenib resistance. (3) Identifying mianserin as a multi-target agent capable of modulating several oncogenic signaling pathways offers broader therapeutic potential than AKT-specific inhibitors. However, this study has certain limitations. *In vivo* validation was limited to a single-dose intratumoral injection strategy, selected to maximize local drug delivery and minimize systemic toxic-

ity. The conventional oral administration route, which holds greater translational relevance due to mianserin's clinical use as an antidepressant, was not assessed in this study. Despite these limitations, our findings offer compelling preclinical evidence for repurposing mianserin as a novel therapeutic option for liver cancer. This work lays a robust foundation for future studies focused on optimizing administration routes, evaluating pharmacokinetics and biodistribution, and designing clinical trials to explore mianserin's full therapeutic potential in liver cancer treatment.

Acknowledgements

This research was funded by Chang Gung Memorial Hospital, Linkou (CMRPD1M0363 to KHL; CMRPG3M0081 and CMRPG3M0082 to YHH; CMRPG3M1263 to CTY; NRRPG3P0011 to YHL); and the National Science and Technology Council, Taiwan (NSTC112-2320-B-182-004 to KHL; NSTC 113-2311-B-182A-001 to YHL).

Disclosure of conflict of interest

None.

Address correspondence to: Dr. Kwang-Huei Lin, Graduate Institute of Biomedical Sciences, College of Medicine, Chang-Gung University, 259 Wen-Hwa 1st Road, Taoyuan, Taiwan. Tel: +886-3-2118263; Fax: +886-3-2118263; E-mail: khlin@mail.cgu.edu.tw; Drs. Yang-Hsiang Lin and Chau-Ting Yeh, Liver Research Center, Chang Gung Memorial Hospital, 5, Fuxing Street, Guishan District, Taoyuan, Taiwan. Tel: +886-3-2118800 Ext. 3559; Fax: +886-3-2118263; E-mail: yhlin0621@cgmh.org.tw (YHL); Tel: +886-3-3281200 Ext. 7799; Fax: +886-3-3282824; E-mail: chautingy@gmail.com (CTY)

References

[1] Philips CA, Rajesh S, Nair DC, Ahamed R, Abduljaleel JK and Augustine P. Hepatocellular carcinoma in 2021: an exhaustive update. Cureus 2021; 13: e19274.

[2] Daher S, Massarwa M, Benson AA and Khoury T. Current and future treatment of hepatocellular carcinoma: an updated comprehensive review. J Clin Transl Hepatol 2018; 6: 69-78.

[3] Yang DK and Kim SJ. Desipramine induces apoptosis in hepatocellular carcinoma cells. Oncol Rep 2017; 38: 1029-1034.

[4] Mun AR, Lee SJ, Kim GB, Kang HS, Kim JS and Kim SJ. Fluoxetine-induced apoptosis in hepatocellular carcinoma cells. Anticancer Res 2013; 33: 3691-3697.

[5] Villanueva-Paz M, Cordero MD, Pavon AD, Vega BC, Cotan D, De la Mata M, Oropesa-Avila M, Alcocer-Gomez E, de Lavera I, Garrido-Maraver J, Carrascosa J, Zaderenko AP, Muntane J, de Miguel M and Sanchez-Alcazar JA. Amitriptyline induces mitophagy that precedes apoptosis in human HepG2 cells. Genes Cancer 2016; 7: 260-277.

[6] Chen VC, Lin CF, Hsieh YH, Liang HY, Huang KY, Chiu WC, Lee Y, McIntyre RS and Chan HL. Hepatocellular carcinoma and antidepressants: a nationwide population-based study. Oncotarget 2017; 8: 30464-30470.

[7] Chan HL, Chiu WC, Chen VC, Huang KY, Wang TN, Lee Y, McIntyre RS, Hsu TC, Lee CT and Tzang BS. SSRIs associated with decreased risk of hepatocellular carcinoma: a population-based case-control study. Psychooncology 2018; 27: 187-192.

[8] Huang YH and Yeh CT. Anticancer effects of antidepressants in hepatocellular carcinoma cells. Anticancer Res 2023; 43: 1201-1206.

[9] Wu SM, Lin SL, Lee KY, Chuang HC, Feng PH, Cheng WL, Liao CJ, Chi HC, Lin YH, Tsai CY, Chen WJ, Yeh CT and Lin KH. Hepatoma cell functions modulated by NEK2 are associated with liver cancer progression. Int J Cancer 2017; 140: 1581-1596.

[10] Schreiber S, Backer MM, Kaufman JP and Pick CG. Interaction between the tetracyclic antidepressant mianserin HCl and opioid receptors. Eur Neuropsychopharmacol 1998; 8: 297-302.

[11] Porsolt RD, Le Pichon M and Jalfre M. Depression: a new animal model sensitive to antidepressant treatments. Nature 1977; 266: 730-732.

[12] Wei JC, Meng FD, Qu K, Wang ZX, Wu QF, Zhang LQ, Pang Q and Liu C. Sorafenib inhibits proliferation and invasion of human hepatocellular carcinoma cells via up-regulation of p53 and suppressing FoxM1. Acta Pharmacol Sin 2015; 36: 241-251.

[13] Chandra D, Choy G and Tang DG. Cytosolic accumulation of HSP60 during apoptosis with or without apparent mitochondrial release: evidence that its pro-apoptotic or pro-survival functions involve differential interactions with caspase-3. J Biol Chem 2007; 282: 31289-31301.

[14] Huang YH and Yeh CT. Functional compartmentalization of HSP60-survivin interaction between mitochondria and cytosol in cancer cells. Cells 2019; 9: 23.

[15] Goh YC, Yap CT, Huang BH, Cronshaw AD, Leung BP, Lai PB, Hart SP, Dransfield I and Ross JA. Heat-shock protein 60 translocates to the surface of apoptotic cells and differentiat-

ed megakaryocytes and stimulates phagocytosis. Cell Mol Life Sci 2011; 68: 1581-1592.
[16] Peng WT, Sun WY, Li XR, Sun JC, Du JJ and Wei W. Emerging roles of g protein-coupled receptors in hepatocellular carcinoma. Int J Mol Sci 2018; 19: 1366.
[17] Zhang Z, Qin C, Wu Y, Su Z, Xian G and Hu B. CCR9 as a prognostic marker and therapeutic target in hepatocellular carcinoma. Oncol Rep 2014; 31: 1629-1636.
[18] Tu Z, Xiao R, Xiong J, Tembo KM, Deng X, Xiong M, Liu P, Wang M and Zhang Q. CCR9 in cancer: oncogenic role and therapeutic targeting. J Hematol Oncol 2016; 9: 10.
[19] Li B, Wang Z, Zhong Y, Lan J, Li X and Lin H. CCR9-CCL25 interaction suppresses apoptosis of lung cancer cells by activating the PI3K/Akt pathway. Med Oncol 2015; 32: 66.
[20] Xu B, Deng C, Wu X, Ji T, Zhao L, Han Y, Yang W, Qi Y, Wang Z, Yang Z and Yang Y. CCR9 and CCL25: a review of their roles in tumor promotion. J Cell Physiol 2020; 235: 9121-9132.
[21] Dong J, Zhai B, Sun W, Hu F, Cheng H and Xu J. Activation of phosphatidylinositol 3-kinase/AKT/snail signaling pathway contributes to epithelial-mesenchymal transition-induced multidrug resistance to sorafenib in hepatocellular carcinoma cells. PLoS One 2017; 12: e0185088.
[22] Tang W, Chen Z, Zhang W, Cheng Y, Zhang B, Wu F, Wang Q, Wang S, Rong D, Reiter FP, De Toni EN and Wang X. The mechanisms of sorafenib resistance in hepatocellular carcinoma: theoretical basis and therapeutic aspects. Signal Transduct Target Ther 2020; 5: 87.
[23] Zheng Y, Chang X, Huang Y and He D. The application of antidepressant drugs in cancer treatment. Biomed Pharmacother 2023; 157: 113985.
[24] Lata S, Mishra R and Banerjea AC. Proteasomal degradation machinery: favorite target of HIV-1 proteins. Front Microbiol 2018; 9: 2738.
[25] Wu SY, Lan SH, Wu SR, Chiu YC, Lin XZ, Su IJ, Tsai TF, Yen CJ, Lu TH, Liang FW, Li CY, Su HJ, Su CL and Liu HS. Hepatocellular carcinoma-related cyclin D1 is selectively regulated by autophagy degradation system. Hepatology 2018; 68: 141-154.
[26] Wei ZL, Zhou X, Lan CL, Huang HS, Liao XW, Mo ST, Wei YG and Peng T. Clinical implications and molecular mechanisms of Cyclin-dependent kinases 4 for patients with hepatocellular carcinoma. BMC Gastroenterol 2022; 22: 77.
[27] Pucci B, Kasten M and Giordano A. Cell cycle and apoptosis. Neoplasia 2000; 2: 291-299.
[28] Sonntag R, Gassler N, Bangen JM, Trautwein C and Liedtke C. Pro-apoptotic sorafenib signaling in murine hepatocytes depends on malignancy and is associated with PUMA expression in vitro and in vivo. Cell Death Dis 2014; 5: e1030.
[29] Li Y, Dowbenko D and Lasky LA. AKT/PKB phosphorylation of p21Cip/WAF1 enhances protein stability of p21Cip/WAF1 and promotes cell survival. J Biol Chem 2002; 277: 11352-11361.
[30] Xu N, Lao Y, Zhang Y and Gillespie DA. Akt: a double-edged sword in cell proliferation and genome stability. J Oncol 2012; 2012: 951724.
[31] Duan Z, Zhou Z, Lu F, Zhang Y, Guo X, Gui C and Zhang H. Antitumor activity of mianserin (a tetracyclic antidepressant) primarily driven by the inhibition of SLC1A5-mediated glutamine transport. Invest New Drugs 2022; 40: 977-989.
[32] Otani K, Kaneko S, Tasaki H and Fukushima Y. Hepatic injury caused by mianserin. BMJ 1989; 299: 519.
[33] Baniel CC, Sumiec EG, Hank JA, Bates AM, Erbe AK, Pieper AA, Hoefges AG, Patel RB, Rakhmilevich AL, Morris ZS and Sondel PM. Intratumoral injection reduces toxicity and antibody-mediated neutralization of immunocytokine in a mouse melanoma model. J Immunother Cancer 2020; 8: e001262.
[34] Bender LH, Abbate F and Walters IB. Intratumoral administration of a novel cytotoxic formulation with strong tissue dispersive properties regresses tumor growth and elicits systemic adaptive immunity in in vivo models. Int J Mol Sci 2020; 21: 4493.
[35] Li W, Dong X, He C, Tan G, Li Z, Zhai B, Feng J, Jiang X, Liu C, Jiang H and Sun X. LncRNA SNHG1 contributes to sorafenib resistance by activating the Akt pathway and is positively regulated by miR-21 in hepatocellular carcinoma cells. J Exp Clin Cancer Res 2019; 38: 183.
[36] Wang H, Tang Y, Yang D and Zheng L. MicroRNA-591 functions as a tumor suppressor in hepatocellular carcinoma by lowering drug resistance through inhibition of far-upstream element-binding protein 2-mediated phosphoinositide 3-Kinase/Akt/Mammalian target of rapamycin axis. Pharmacology 2019; 104: 173-186.
[37] Zhai B, Hu F, Jiang X, Xu J, Zhao D, Liu B, Pan S, Dong X, Tan G, Wei Z, Qiao H, Jiang H and Sun X. Inhibition of Akt reverses the acquired resistance to sorafenib by switching protective autophagy to autophagic cell death in hepatocellular carcinoma. Mol Cancer Ther 2014; 13: 1589-1598.
[38] Xing Y, Lin NU, Maurer MA, Chen H, Mahvash A, Sahin A, Akcakanat A, Li Y, Abramson V, Litton J, Chavez-MacGregor M, Valero V, Piha-Paul SA, Hong D, Do KA, Tarco E, Riall D, Eterovic AK, Wulf GM, Cantley LC, Mills GB, Doyle LA, Winer E, Hortobagyi GN, Gonzalez-Angulo AM

and Meric-Bernstam F. Phase II trial of AKT inhibitor MK-2206 in patients with advanced breast cancer who have tumors with PIK3CA or AKT mutations, and/or PTEN loss/PTEN mutation. Breast Cancer Res 2019; 21: 78.

[39] Myers AP, Konstantinopoulos PA, Barry WT, Luo W, Broaddus RR, Makker V, Drapkin R, Liu J, Doyle A, Horowitz NS, Meric-Bernstam F, Birrer M, Aghajanian C, Coleman RL, Mills GB, Cantley LC, Matulonis UA and Westin SN. Phase II, 2-stage, 2-arm, PIK3CA mutation stratified trial of MK-2206 in recurrent endometrial cancer. Int J Cancer 2020; 147: 413-422.

[40] Hua H, Zhang H, Chen J, Wang J, Liu J and Jiang Y. Targeting Akt in cancer for precision therapy. J Hematol Oncol 2021; 14: 128.

[41] Mroweh M, Roth G, Decaens T, Marche PN, Lerat H and Macek Jílková Z. Targeting akt in hepatocellular carcinoma and its tumor microenvironment. Int J Mol Sci 2021; 22: 1794.

[42] Berard R, Wood L and Viljoen G. Mianserin in oncology: the issue of psychotropic-related neutropenia. Psycho-Oncology 1993; 2: 219-222.

[43] Fiscon G, Conte F, Amadio S, Volonté C and Paci P. Drug repurposing: a network-based approach to amyotrophic lateral sclerosis. Neurotherapeutics 2021; 18: 1678-1691.

[44] Okura T, Ohkawara B, Takegami Y, Ito M, Masuda A, Seki T, Ishiguro N and Ohno K. Mianserin suppresses R-spondin 2-induced activation of Wnt/β-catenin signaling in chondrocytes and prevents cartilage degradation in a rat model of osteoarthritis. Sci Rep 2019; 9: 2808.

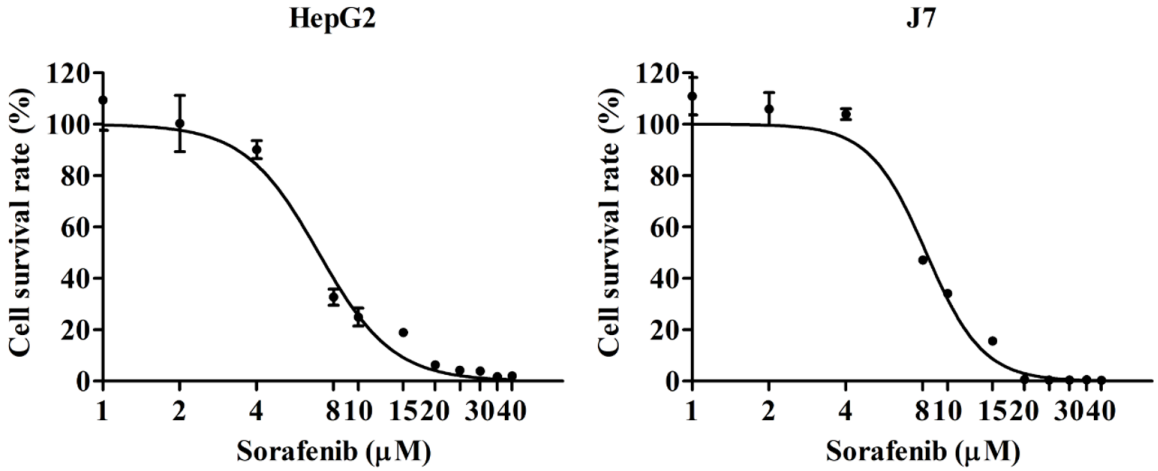

Figure S1. IC50 values of liver cancer cell lines. Cells were seeded and cultured overnight to allow adhesion. Sorafenib was applied at concentrations ranging from 0 to 40 μM, and cell survival rates were assessed after 3 days using the MTT assay. The IC50 values were calculated based on the dose-response curve, representing the concentration of sorafenib required to inhibit 50% of cell viability.

Table S1. Quantification results (mean ± SD) of Western blot

Figure 1B								
Target	Lane 1	Lane 2	Lane 3	Lane 4				
Cyclin D1	1	0.12 ± 0.12$^{***,\#1}$	1	0.18 ± 0.21**				
CDK4	1	0.38 ± 0.26**	1	0.66 ± 0.22*				
Figure 3A								
Target	Lane 1	Lane 2	Lane 3	Lane 4	Lane 5	Lane 6	Lane 7	Lane 8
HSP60	1	0.65 ± 0.13	1	1.24 ± 0.04*	1	0.23 ± 0.08**	1	0.85 ± 0.12
Figure 3B								
Target	Lane 1	Lane 2	Lane 3	Lane 4				
sHSP60	1	1.26 ± 0.11***	1	1.93 ± 0.00***				
CCR9	1	0.71 ± 0.27*	1	0.54 ± 0.19*				
Figure 3C								
Target	Lane 1	Lane 2	Lane 3	Lane 4				
CCR9	1	1.48 ± 0.45	1	1.94 ± 0.51				
Figure 4B								
Target	Lane 1	Lane 2	Lane 3	Lane 4	Lane 5	Lane 6	Lane 7	Lane 8
sHSP60	1$^{a,\#2}$	1.17 ± 0.08^{b}	0.76 ± 0.03$^{a'b'c}$	1.06 ± 0.07$^{c'}$	1^{d}	1.31 ± 0.06$^{d'e}$	0.72 ± 0.06$^{d'e'}$	0.85 ± 0.10$^{e'}$
CCR9	1	0.56 ± 0.10	1.04 ± 0.20	1.06 ± 0.27	1	0.67 ± 0.19	1.05 ± 0.07	0.89 ± 0.23
Figure 5A								
Target	Lane 1	Lane 2	Lane 3	Lane 4				
AKT	1	0.81 ± 0.24	1	0.81 ± 0.05*				
p-AKT	1	0.37 ± 0.23**	1	0.54 ± 0.27**				
β-catenin	1	0.42 ± 0.10***	1	0.56 ± 0.29**				
NFκB	1	0.54 ± 0.12***	1	0.59 ± 0.22**				
Figure 5B								
Target	Lane 1	Lane 2	Lane 3	Lane 4	Lane 5	Lane 6	Lane 7	Lane 8
p-AKT	1^{a}	0.95 ± 0.02	0.47 ± 0.20$^{a'}$	0.62 ± 0.15	1^{b}	0.85 ± 0.14^{c}	0.38 ± 0.21$^{b'c'}$	0.49 ± 0.15$^{b'c'}$
β-catenin	1^{a}	0.75 ± 0.01^{b}	0.40 ± 0.07$^{a'b'}$	0.51 ± 0.09$^{a'b'}$	1	0.99 ± 0.12	0.41 ± 0.18	0.55 ± 0.27
NFκB	1	0.72 ± 0.19	0.47 ± 0.15	0.62 ± 0.17	1^{a}	0.91 ± 0.04^{b}	0.47 ± 0.06$^{a'b'c}$	0.57 ± 0.08$^{a'b'c'}$

Figure S2

Target	Lane 1	Lane 2	Lane 3	Lane 4	Lane 5	Lane 6	Lane 7	Lane 8
CCR9	1	0.67 ± 0.07	0.53 ± 0.01	0.21 ± 0.06	0.97 ± 0.41	0.84 ± 0.32	1.36 ± 0.79	0.72 ± 0.26
AKT	1[a]	0.95 ± 0.05	0.79 ± 0.04	0.72 ± 0.12[a']	0.80 ± 0.02	0.70 ± 0.02	0.91 ± 0.07	0.68 ± 0.08
p-AKT	1[a]	0.30 ± 0.02	2.11 ± 0.01[a'b]	0.56 ± 0.10[b']	1.79 ± 0.48[c]	0.36 ± 0.02[c'd]	2.56 ± 0.60[d'e]	0.20 ± 0.04[c'e']
β-catenin	1	0.85 ± 0.06	0.83 ± 0.00	0.47 ± 0.05	2.07 ± 0.29	2.09 ± 0.20	2.59 ± 0.20	2.18 ± 0.27
NFκB	1[a]	0.78 ± 0.07[b]	0.57 ± 0.09[a']	0.38 ± 0.02[a'b']	0.07 ± 0.03[a']	0.10 ± 0.07	0.24 ± 0.10	0.12 ± 0.11
Target	Lane 9	Lane 10	Lane 11	Lane 12	Lane 13	Lane 14	Lane 15	Lane 16
CCR9	1	1.13 ± 0.02	1.03 ± 0.42	0.33 ± 0.36	1.14 ± 0.37	0.52 ± 0.35	1.11 ± 0.03	0.25 ± 0.26
AKT	1[a]	0.76 ± 0.12	0.53 ± 0.13	0.16 ± 0.01[a']	0.56 ± 0.33	0.52 ± 0.10	1.23 ± 0.31	0.31 ± 0.25
p-AKT	1[a]	0.38 ± 0.22	0.42 ± 0.18	0.21 ± 0.17[a']	0.52 ± 0.33[b]	0.47 ± 0.06[c]	1.43 ± 0.21[b'c'd]	0.43 ± 0.03[d']
β-catenin	1	0.81 ± 0.12	1.92 ± 1.12	0.63 ± 0.05	1.31 ± 0.20	0.37 ± 0.22	2.16 ± 1.31	0.62 ± 0.25
NFκB	1	0.45 ± 0.42	1.26 ± 0.13	0.49 ± 0.24	1.43 ± 0.16[a]	0.82 ± 0.37	1.14 ± 0.17	0.19 ± 0.27[a']

#1, Student's t-test was used to compare two groups, while one-way ANOVA and Tukey's multiple comparison test were used to compare groups with more than two; *, $P<0.05$; **, $P<0.01$; ***, $P<0.001$; #2, multiple comparisons were conducted between groups with the same letter; an apostrophe indicates statistical significance.

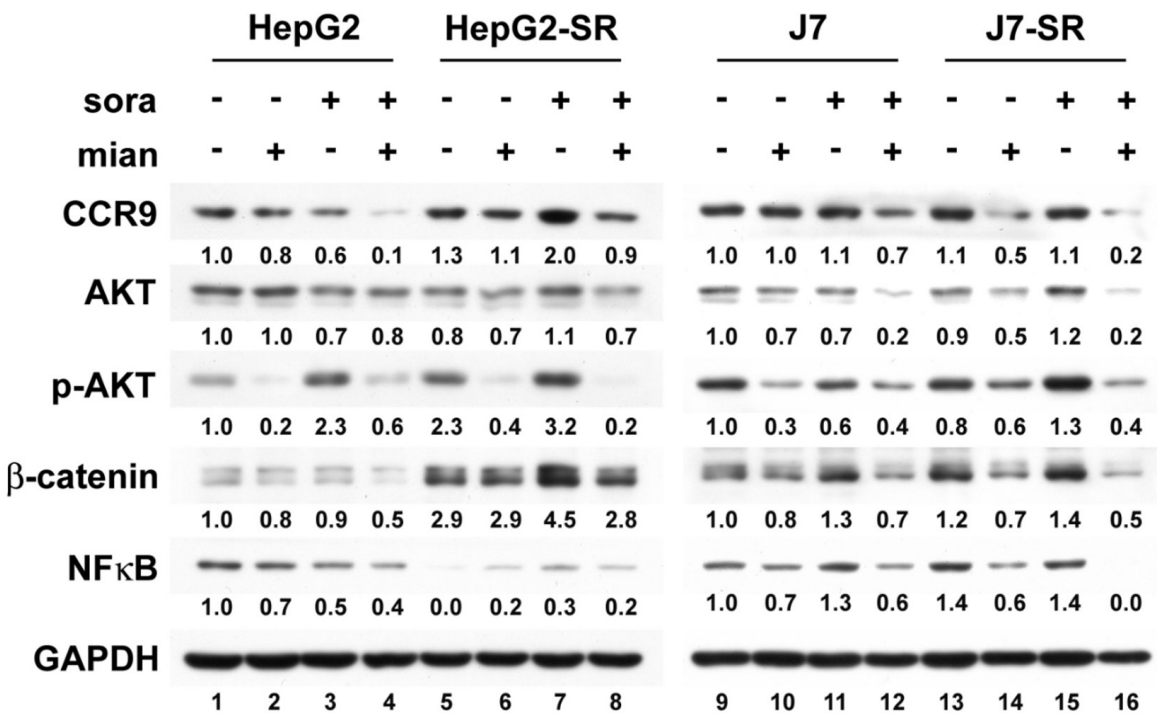

Figure S2. Effects of mianserin and sorafenib, alone or in combination, on the CCR9-AKT pathway in parental and sorafenib-resistant (SR) cancer cells. HepG2 and HepG2-SR cells were treated with mianserin (20 μg/mL) and sorafenib (5 μM), either alone or in combination, for 24 h. J7 and J7-SR cells were treated with mianserin (15 μg/mL) and sorafenib (5 μM), either alone or in combination, for 46 h. Total proteins were extracted for immunoblot analysis. Quantifications of the bands from the representative images are shown.